FUZZY LOGIC BASED CONTROLLER FOR A STAND-ALONE HYBRID GENERATION SYSTEM USING WIND AND PHOTOVOLTAIC ENERGY

G. Balasubramanian[1] and S. Singaravelu[2]
[1]Department of Electrical Engineering, Annamalai University, Annamalainagar, India

ABSTRACT

Fuzzy logic based voltage controller is proposed for hybrid generation scheme using solar and wind energy for isolated applications. The fuzzy logic controller is designed to vary the duty-cycle of the DC-DC converter automatically such that to maintain the load voltage constant. The hybrid scheme comprises one set of fixed capacitor bank and a parallel connected three-phase fixed frequency pulse width modulation (PWM) inverter fed from the solar panels which provide the reactive power requirements to the induction generator. A dynamic d-q axis and steady-state mathematical model for the entire hybrid scheme is presented. The complete system is modelled and simulated MATLAB/Simulink environment. Results from simulations and laboratory tests show that the dynamic reactive power compensation is inherent.

KEYWORDS: *Hybrid, Solar, Induction Generator, DC-DC Converter & Inverter.*

I. INTRODUCTION

The rapid growth in power electronics techniques makes the feasibility in hybrid scheme generation using wind and photovoltaic system [1]. The renewable energy systems can be used to supply power either directly to a utility grid or to an isolated load. The stand-alone systems find wider application as water-pumps, for village electrification, supply of power to isolated areas which are far away from the utility grid [2]. Generally, PV power and wind power are complementary since sunny days are usually calm and strong winds often occur on cloudy days or in night time. The hybrid PV-wind power system therefore has higher availability to deliver continuous power and results in a better utilization of power conversion and control equipment than with of the individual sources [3]. Further hybrid PV-wind scheme has environmental benefits such as reduction of carbon emission due to use of renewable energy sources [4]. In case of stand-alone wind power generation system with a self-excited induction generator, it is necessary to provide a dynamically variable reactive power to maintain constant output voltages [5-8]. But in case of solar-wind hybrid scheme the necessary reactive power under varying rotor speed or load can be achieved by providing a three-phase fixed frequency pulse width modulation (PWM) inverter fed from the photovoltaic array. In this paper fuzzy logic controller is designed to vary the duty-cycle of the DC-DC converter such that to maintain the load voltage constant under varying rotor speeds or loads.

The paper is arranged as follows: Section II describes the entire hybrid scheme for solar and wind energy conversion. Section III explains the photo-voltaic, dynamic and the steady-state modeling. Section IV and V describes the DC-DC converter and the proposed fuzzy logic controller. Section VI discusses the results of the hybrid scheme and the conclusions from the study are given in Section VII.

II. HYBRID SCHEME DESCRIPTION

Fig. 1 describes the hybrid scheme of solar-wind with the proposed fuzzy logic controller. A self-excited induction generator (SEIG) connected in parallel with the inverter. The base level excitation requirement is provided by one fixed capacitor bank. The additional excitation requirements under varying rotor speed or load is supplied by the parallel connected inverter fed by solar array.

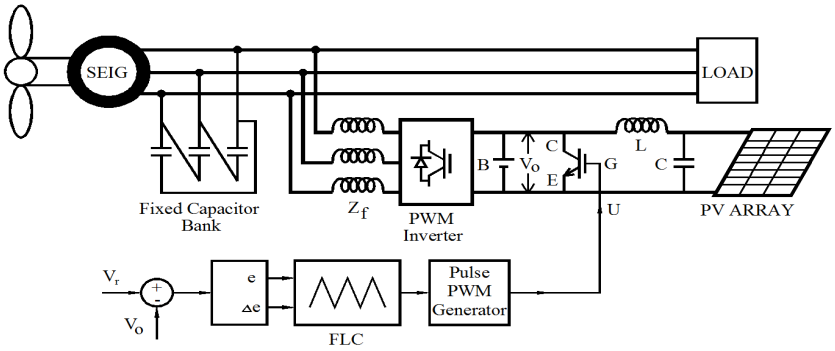

Figure 1. Schematic diagram of solar-wind hybrid scheme

Whenever the wind speed is lower than the nominal synchronous speed or at higher load, the SEIG generates less than the rated voltage if no parallel inverter. But in the proposed hybrid scheme due to the presence of parallel connected inverter fed by battery which is charged by the photovoltaic array will provide the necessary additional lagging reactive power to the SEIG to develop the rated voltage. At the same time the battery will supply a small amount of real power through inverter. Whenever the wind speed near to the synchronous speed or beyond, the real power supplied by the inverter decreases in magnitude. At the same time, the reactive power supplied by the inverter is also decreases because of the fixed capacitor bank. Thus the inverter supplies the balance reactive power (difference in fixed capacitance var and the actual requirement) at the given speed and load condition. Also the battery connected to the inverter supplied a limited real power. At the same time the generator frequency is tied to the inverter output frequency. The above said can be achieved by the proposed fuzzy logic controller which varies the duty cycle of DC-DC step up converter automatically. This proves the self-regulating mechanism of the proposed scheme.

III. MODELING OF HYBRID SCHEME

The solar array equivalent circuit, d-axis and q-axis equivalent circuit and steady-state equivalent circuit of the hybrid scheme is presented in this section. The dynamic and steady-state behaviour of the hybrid scheme under varying rotor speed and load can be predicted using the equivalent circuits.

3.1. PV array model

Fig.2 shows the equivalent circuit of PV cell.

A PV cell can be represented by an equivalent circuit [9] as shown in Fig. 2. The characteristics of this PV cell can be obtained using standard equation (1).

$$I = I_{PV} - I_O \left[\exp\left(\frac{V+R_S I}{V_t a}\right) - 1\right] - \frac{V+R_S I}{R_p} \quad (1)$$

I_{PV} = photovoltaic current
I_O = saturation current
V_t = N_S k T/q, thermal voltage of array
Ns = cell connected in series
T = is the temperature of the p-n junction
k = Boltzmann constant
q = electron charge
R_S = equivalent series resistance of the array

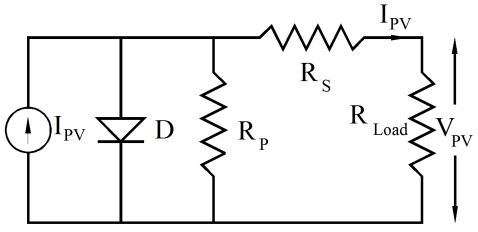

Figure 2: Equivalent circuit of PV cell

R_P = equivalent parallel resistance of the array
a = diode ideality constant

Fig. 1 shows the single diode model. A single solar cell will produce only a limited power. Therefore it is usual practice in order to get desired power rating the solar cells are connected in parallel and series circuits which form a module. Such modules are again connected in parallel and series to form a solar array or panel to get required voltage and current. The equivalent series and parallel resistance of the array are denoted by the symbol R_S and R_P respectively in the equivalent circuit.

From the general *I-V* characteristic of the practical photovoltaic device one can observe that the series resistance R_S value will dominate in the voltage source region and the parallel resistance R_P value will dominate in the current source region of operation.

The general equation of a PV cell describes the relationship between current and voltage of the cell. Since the value of shunt resistance R_P is high compared to value of series resistance R_S the current through the parallel resistance can be neglected. The light generated current of the photovoltaic cell depends linearly on the solar irradiation and is also influenced by the temperature [10] given by the equation (2)

$$I_{PV} = \left[I_{PV,n} + K_I \Delta_T\right] \frac{G}{G_n} \quad (2)$$

$I_{PV,n}$= is the light generated current at nominal condition(25^0C and 1000 W/ m^2)
Δ_T = $T - T_n$
T = actual temperature [K]
T_n = nominal temperature [K]
K_I = current coefficients
G = irradiation on the device surface [W/m^2]
G_n = nominal irradiation

The current and voltage coefficients K_V and K_I are included as shown in equation (3) in order to take the saturation current I_O which is strongly dependent on the temperature.

$$I_O = \frac{I_{sc,n} + K_I \Delta_T}{exp\left(\frac{V_{oc,n} + K_V \Delta_T}{a V_t}\right) - 1} \quad (3)$$

K_V = voltage coefficients
K_I = current coefficients

The output voltage is increased (where the current remain unchanged) proportionally on number of identical PV modules connected in series (N_{ser}). Similarly the output current is increased (where the voltage remain unchanged) proportionally on number of identical PV modules connected in parallel (N_{par}).

It can be noted that the equivalent series and parallel resistance are directly proportional to the number of series modules and inversely proportional to the number of parallel modules respectively.

The equation for array composed of N_{ser} x N_{par} given by equation (4)

$$I = I_{PV} N_{par} - I_O N_{par} \left[\exp\left(\frac{V + R_S\left(\frac{N_{ser}}{N_{par}}\right) I}{V_t a N_{ser}}\right) - 1\right] - \frac{V + R_S\left(\frac{N_{ser}}{N_{par}}\right) I}{R_P\left(\frac{N_{ser}}{N_{par}}\right)} \quad (4)$$

Table 1. Parameter of KCP -12075 solar array at 25℃, 1000W/m^2

I_{mp}	4.40 A	V_{oc}	21.20 V
V_{mp}	17.00 V	a	1.3
P_{max}	74.8 W	R_{se}	0.511 Ω
I_{sc}	5.02 A	R_{sh}	44.25 Ω
N_s	36	K_v	-74.7 mv/℃
$I_{O,n}$	9.83 x 10^{-8}A	K_I	2.80 mA/℃

3.2. Dynamic Modelling

Fig.3 shows the d-axis and q-axis equivalent circuit of the hybrid scheme. The differential equations governing the stator and rotor currents in stator flux reference frame of the induction machine can be written as follows [11].

$$L_s \frac{d}{dt}(i_{sq}) = v_{sq} - R_s\, i_{sq} - (\omega_{ms})(L_s i_{sd} + L_o i_{rd}) - L_o \frac{d}{dt}(i_{rq}) \quad (5)$$

$$L_s \frac{d}{dt}(i_{sd}) = v_{sd} - R_s\, i_{sd} + (\omega_{ms})\left(L_s i_{sq} + L_o i_{rq}\right) - L_o \frac{d}{dt}(i_{rd}) \quad (6)$$

$$L_r \frac{d}{dt}(i_{rq}) = v_{rq} - R_r\, i_{rq} + (\omega_{ms} - \omega_e)(L_r i_{rd} + L_o i_{sd}) - L_o \frac{d}{dt}(i_{sq}) \quad (7)$$

$$L_r \frac{d}{dt}(i_{rd}) = v_{rd} - R_r\, i_{rd} + (\omega_{ms} - \omega_e)\left(L_r i_{rq} + L_o i_{sq}\right) - L_o \frac{d}{dt}(i_{sd}) \quad (8)$$

The modeling of the excitation system are given below

$$\frac{d}{dt}(v_{sd}) = 1/C(i_{sd} - i_{Ld} + i_d\ ) + \ \omega_{ms} v_{sq} \quad (9)$$

$$\frac{d}{dt}(v_{sq}) = 1/C(i_{sq} - i_{Lq} + i_q\ ) - \ \omega_{ms} v_{sd} \quad (10)$$

The modeling of Inverter – dc-dc converter - battery system

$$\frac{d}{dt}(i_{id}) = 1/L_f(v_{id} - R_f - v_{sd}) + \ \omega_{ms} i_{iq} \quad (11)$$

$$\frac{d}{dt}(i_{iq}) = 1/L_f(v_{iq} - R_f - v_{sq}) \ - \ \omega_{ms} i_{id} \quad (12)$$

The modeling of resistive load

$$\frac{v_{sd}}{R_L} = \ i_{Ld} \text{ and } \frac{v_{sq}}{R_L} = \ i_{Lq} \quad (13)$$

where,

$$\Psi_{sq} = -L_{ls} i_{sq} - L_m\left(i_{rq} + i_{sq}\right), \Psi_{sd} = -L_{ls} i_{sd} - L_m(i_{rd} + i_{sd})$$
$$\Psi_{rd} = -L_{lr} i_{rd} - L_m(i_{rd} + i_{sd}) and \Psi_{rq} = -L_{lr} i_{rq} - L_m\left(i_{rq} + i_{sq}\right)$$

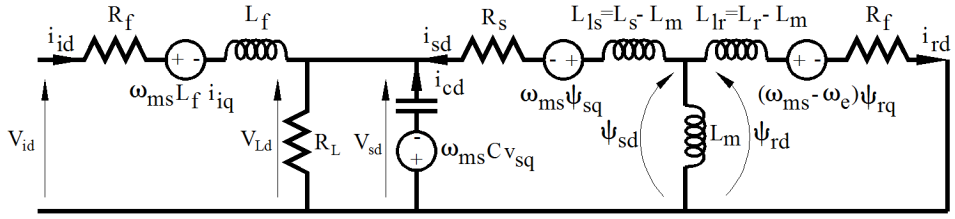

(a) d-axis model

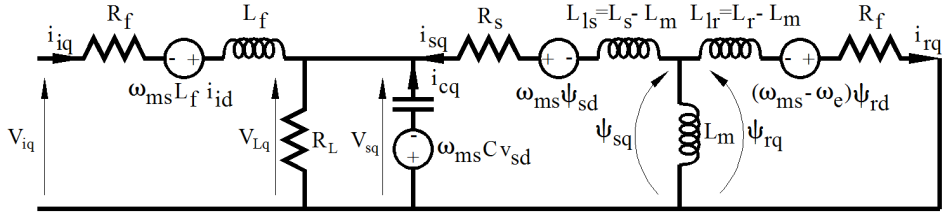

(b) q-axis model

Figure 3. d-axis and q-axis equivalent circuit

3.3. Steady-State modelling

Fig.4 shows the per-phase steady-state equivalent circuit [12] of the of the hybrid scheme. The mathematical model is developed using nodal admittance by the method of inspection. Since the developed model is in matrix form which makes the analysis simple.

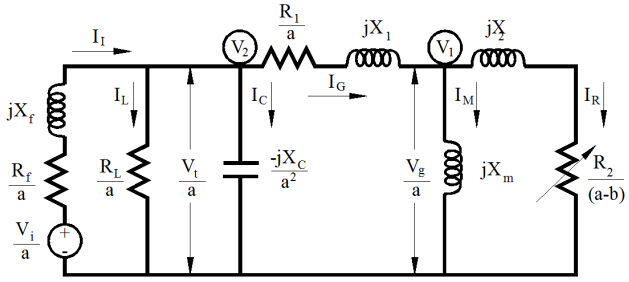

Figure 4. Per-phase equivalent circuit of the system

The various elements of the equivalent circuit (Fig. 4) is given below

$$Z_f = \frac{R_f}{a} + jX_f \qquad Z_s = \frac{R_1}{a} + jX_1 \qquad Z_L = \frac{R_L}{a}$$

$$Z_R = \frac{R_2}{a-b} + jX_2 Z_c = 0 - j\frac{X_c}{a^2} \qquad Z_M = 0 + jX_m \tag{14}$$

The various branch currents of the equivalent circuit (Fig. 4) is given below

$$I_i = (V_i/a - V_2)/Z_f \qquad I_L = (V_2)/Z_L$$

$$I_C = (V_2)/Z_C \qquad I_g = (V_2 - V_1)/Z_s$$

$$I_m = (V_1)/Z_m \qquad I_r = (V_1)/Z_R \tag{15}$$

From Figure 4 the node equations can be written as follows

At node 1 (V_1), the Kirchhoff's Current Law equation can be written as

$$I_g = I_r + I_m \tag{16}$$

By substituting the values of I_g, I_r and I_m in equation (16) and rearranging we get

$$V_1\left(\frac{1}{Z_R} + \frac{1}{Z_m} + \frac{1}{Z_s}\right) - V_2\left(\frac{1}{Z_s}\right) = 0 \tag{17}$$

At node 2 (V_2), the Kirchhoff's Current Law equation can be written as

$$I_i = I_L + I_C + I_g \tag{18}$$

By substituting the values of I_i, I_L, I_C and I_g in equation (18) and rearranging we get

$$\frac{\frac{V_i}{a} - V_2}{Z_f} = \frac{V_2}{Z_L} + \frac{V_2}{Z_C} + \frac{V_2 - V_1}{Z_s} - V_1\left(\frac{1}{Z_s}\right) + V_2\left(\frac{1}{Z_L} + \frac{1}{Z_C} + \frac{1}{Z_f} + \frac{1}{Z_s}\right) = \frac{V_i}{a}\left(\frac{1}{Z_f}\right) \tag{19}$$

The equations (17) and (19) can be written in matrix from as follows

$$\begin{bmatrix} \frac{1}{Z_R} + \frac{1}{Z_m} + \frac{1}{Z_s} & -\frac{1}{Z_s} \\ -\frac{1}{Z_s} & \frac{1}{Z_L} + \frac{1}{Z_C} + \frac{1}{Z_f} + \frac{1}{Z_s} \end{bmatrix} \begin{bmatrix} V_1 \\ V_2 \end{bmatrix} = \begin{bmatrix} 0 \\ \frac{\left(\frac{V_i}{a} - V_2\right)}{Z_f} \end{bmatrix} \tag{20}$$

The equation (20) is in matrix form which can be utilized to find the steady state analysis.

IV. DC – DC BOOST CONVERTER

A dual stage power electronic system comprising a boost type dc-dc converter and an inverter is used to feed the power generated by the PV array to the load.To maintain the load voltage constant a DC-DC step up converter is introduced between the PV array and the inverter. The block schematic of the proposed scheme is shown in Fig. 1. In this scheme a PV array feeds DC-DC converter used in step-up configuration. The voltage across the DC-DC converter is fed to a three-phase, six-step, quasi-square-wave IGBT inverter a three-phase fixed amplitude and fixed frequency supply is obtained to feed an isolated load. For a dc-dc boost converter, by using the averaging concept, the input–output voltage relationship for continuous conduction mode is given by

$$Vo/Vin = 1/(1 - D) \tag{21}$$

Where, D = duty cycle. Since the duty ratio "D" is between 0 and 1 the output voltage must be higher than the input voltage in magnitude. It should be noted that the control logic of such dc-dc converter has to be different when it is fed from a stiff DC source. The duty ratio of the chopper is found to increase linearly with increase in cell temperature and hence the intensity.

As the inverter DC voltage varies with irradiation to obtain constant amplitude and constant frequency supply from the inverter, a closed loop fuzzy controller is incorporated to automatically vary the duty-cycle of the DC-DC converter to obtain constant DC voltage at the inverter input terminals. The inverter output is then applied to an isolated load. At the same time fuzzy controller will maintain the output voltage of inverter by supplying the required reactive power according to the change in speed of the wind and load. This can be achieved by maintaining the battery voltage adequately high.

V. FUZZY LOGIC MPPT CONTROLLERS

The conventional PI controllers are fixed-gain feedback controllers. Therefore they cannot compensate the parameter variations in the process and cannot adapt changes in the environment. PI-controlled system is less responsive to real and relatively fast alterations in state and so the system will be slower to reach the set point. On the other hand P&O method for MPPT tracking will not respond quickly to rapid changes in temperature or irradiance. Therefore the fuzzy control algorithm is capable of improving the tracking performance as compared with the classical methods for both linear and nonlinear loads. Also, fuzzy logic is appropriate for nonlinear control because it does not use complex mathematical equation. The two FLC input variables are the error E and change of error ΔE. The behavior of a FLC depends on the shape of membership functions of the rule base. In this paper a fuzzy logic control scheme (Fig.5) is proposed for maximum solar power tracking of the PV array with an inverter for supplying isolated loads. They have advantages to be robust and relatively simple to design since they do not require the knowledge of the exact model. On the other hand the designer needs complete knowledge of the hybrid system operation.

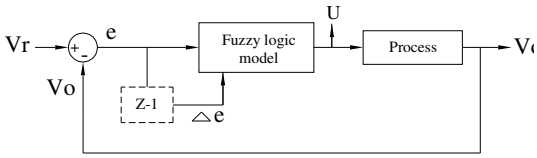

Figure 5: Fuzzy logic control scheme

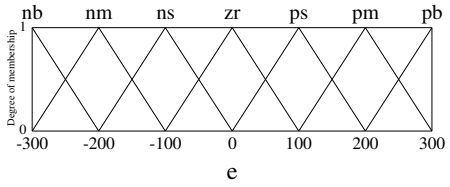

Figure 6 (a): Membership function plots for 'e'

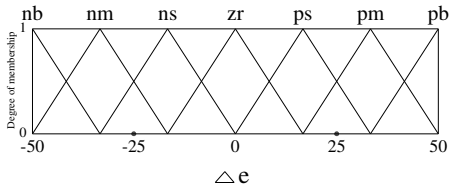

Figure 6(b): Membership function plots for 'Δe'

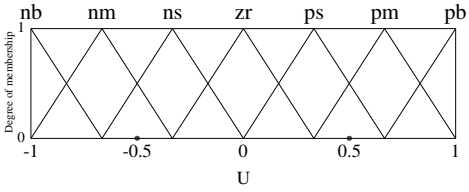

Figure 6(c): Membership function plots for 'U'

Fig 6 Membership function

5.1. Fuzzification

The membership function values are assigned to the linguistic variables using seven fuzzy subset called negative big (nb), negative medium (nm), negative small (ns), zero(zr), positive small (ps), positive medium (pm), positive big (pb). Fuzzy associative memory for the proposed system is given in Table-2. Variable e and Δe are selected as the input variables, where e is the error between the reference voltage (Vr) and actual voltage (Vo) of the system, Δe is the change in error in the sampling interval. The output variable is the reference signal for PWM generator U. Triangular membership functions are selected for all these process. The range of each membership function is decided by the previous knowledge of the proposed scheme parameters.

5.2. Inference engine

Inference engine mainly consist of Fuzzy rule base and fuzzy implication sub blocks. The inputs are now fuzzified are fed to the inference engine and the rule base is then applied. The output fuzzy set are then identified using fuzzy implication method. Here we are using MIN-MAX fuzzy implication method.

Table2. Fuzzy associative memory for the proposed system

e	Δe						
	nb	nm	ns	zr	ps	pm	pb
nb	nb	nb	nb	nm	nm	ns	zr
nm	nb	nb	nm	nm	ns	zr	ps
ns	nb	nm	nm	ns	zr	ps	pm
zr	nm	nm	ns	zr	ps	pm	pm
ps	nm	ns	zr	ps	pm	pm	pb
pm	ns	zr	ps	pm	pm	pb	pb
pb	zr	ps	pm	pm	pb	pb	pb

5.3. Defuzzification

Once fuzzification is over, output fuzzy range is located. Since at this stage a non-fuzzy value of control is available a defuzzification stage is needed. Centroid defuzzification method [13] is used for defuzzification in the proposed scheme.
The membership function of the variables error, change in error and change in reference signal for PWM generator are shown in Fig. 6a-6c respectively.

VI. RESULTS AND DISCUSSIONS

A MATLAB based modeling and simulation scheme (Appendix) with fuzzy logic controller is proposed which are suitable for studying performance of the hybrid scheme (Fig.1). The experimental setup and machine parameters details are also given in Appendix. The photovoltaic *I-V* and *P-V* characteristics are discussed. Also, the steady-state and dynamic characteristics of the hybrid scheme under varying speed and load conditions are discussed.

6.1. PV-characteristics

The behaviour the PV cells and its characteristics are discussed in this section. It is found that the set of *P-V*&*I*-V characteristics are highly nonlinear and dependent on solar irradiance of the PV array.

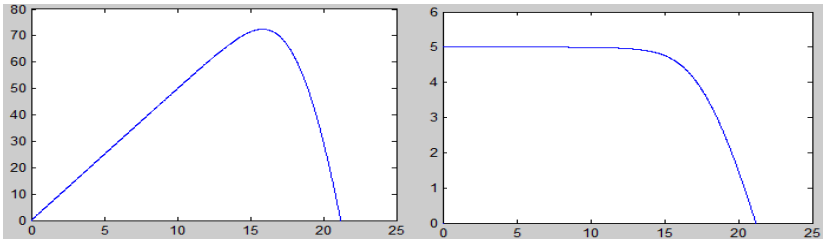

Figure7(a): P-V Characteristics **Figure7(b):** I-V Characteristics

Figure 7(a) and 7(b) shows P-V and I-V characteristics of a PV cell. It can be observed that as the cell temperature remain constant the PV output voltage remains nearly constant while the PV output current increases with increasing solar intensity.

6.2. Steady-state performance of the hybrid scheme

The per-phase equivalent circuit is shown in Fig. 4. A new mathematical model for the steady-state analysis in matrix form (equation 20) is presented in section 3.3. The steady state model includes the equivalent circuit of the inverter and its impedance of the inverter side filter. The steady-state characteristics under varying rotor speed of the SEIG from 1400 to 1700 rpm and minimum to maximum irradiation from 0.3 to 0.9 kW/m^2 of the PV cell are discussed.

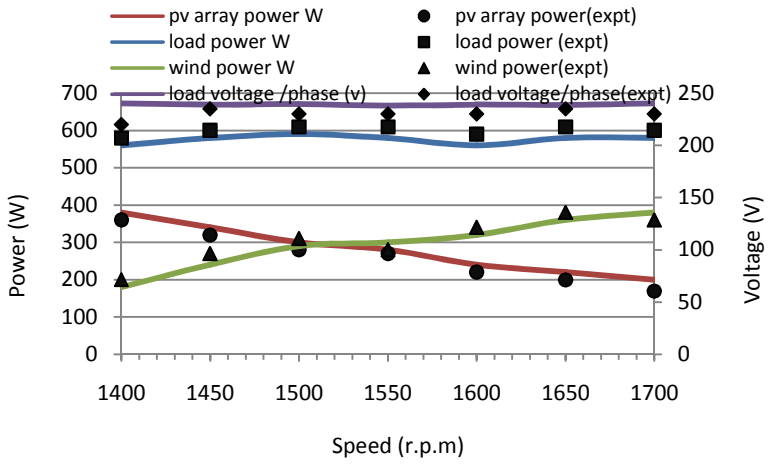

Figure. 8(a) Minimum irradiation and varying wind speed

Figure 8(a) shows wind speed variation from 1400 to 1700 rpm at minimum solar irradiation of 0.3kW/m^2. When the wind speed is around 1400 rpm (below synchronous speed) the PV array power increases (by proportionally varying the duty cycle of DC-DC converter) and supplies the additional power to the load through the inverter and hence the load voltage is maintained as desired. On the other hand when the wind speed is around 1550 rpm (above synchronous speed) the SEIG will supply directly the additional power to the load and hence the load voltage is maintained as desired wherein

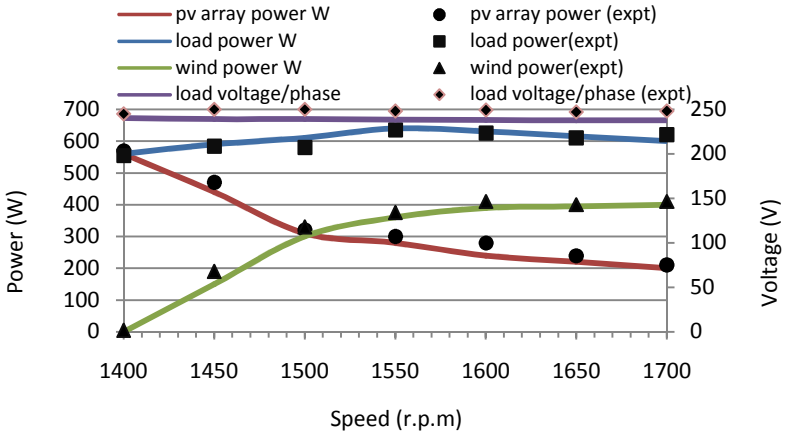

Figure. 8(b) Maximum irradiation and varying wind speed

the PV array power decreases.

Figure 8(b) shows wind speed variation from 1400 to 1700 rpm at maximum solar irradiation of 0.9kW/m^2. When the wind speed is around 1400 rpm (below synchronous speed) since the solar irradiation is maximum the PV array power increases and supplies the additional power to the load through the inverter and hence the load voltage is maintained as desired. On the other hand when the wind speed is around 1550 rpm (above synchronous speed) the SEIG will supply directly the additional power to the load and hence the load voltage is maintained as desired wherein the PV array power decreases (by proportionally varying the duty cycle of DC-DC converter).

Figure 8(c) shows variation of solar irradiation from 0.3 to 0.9kW/m^{2}at minimum wind speed of 1400rpm. When the irradiation is minimum of 0.3kw/m^{2}the PV array power has to be increased by proportionally varying the duty cycle of DC-DC converter. Thus the additional power will be supplied by the PV array through the inverter to the load and hence the load voltage is maintained as desired. On the other hand when the irradiation is maximum of 0.9kw/m^{2}the PV array power directly supplies the additional power to the load and hence the load voltage is maintained as desired.

Figure 8(d) shows variation of solar irradiation from 0.3 to 0.9kW/m^{2}at maximum wind speed of 1700rpm. When the irradiation is minimum of 0.3kw/m^{2}the SEIG will directly supplies the additional power to the load and hence the load voltage is maintained as desired. On the other hand when the

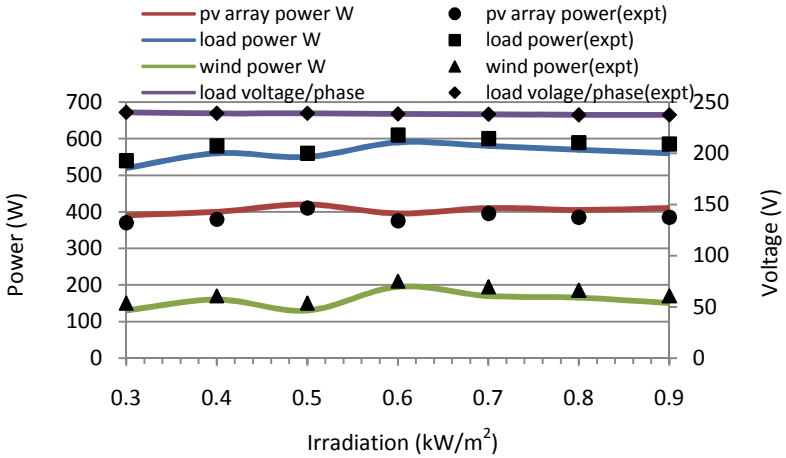

Figure. 8(c) Minimum wind speed and varying irradiation

irradiation is maximum of 0.9kw/m^{2}the PV array power has to decreased by proportionally varying the duty cycle of DC-DC converter the SEIG still supplies the additional power to the load and hence the load voltage is maintained as desired.

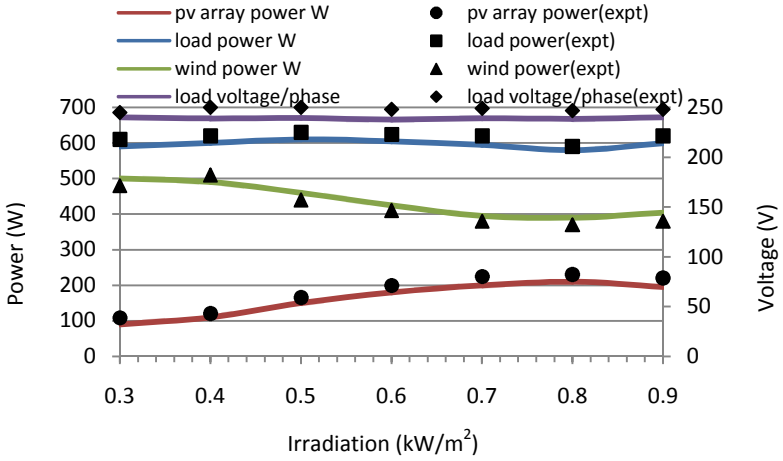

Figure. 8(d) Maximum wind speed and varying irradiation

The above said can be achieved by the proposed fuzzy logic controller which varies the duty cycle of DC-DC step up converter automatically. This proves the self-regulating mechanism of the proposed scheme.

6.2. Dynamic response of the hybrid scheme

The simulated per phase voltage and current waveform across the load is shown in Fig. 9(a). The simulated per phase current waveform (Fig. 9(b)) shows, even though the load is applied at 0.8 seconds the voltage across the load remains constant. Figure 9(c) and 9(d) shows the experimental waveforms.Some harmonics have been introduced in the proposed scheme found in the waveforms it can be eliminated by introducing necessary filters.

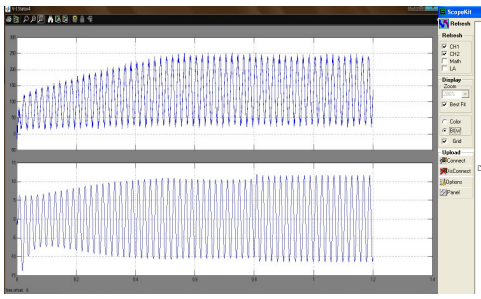

Figure 9(a).

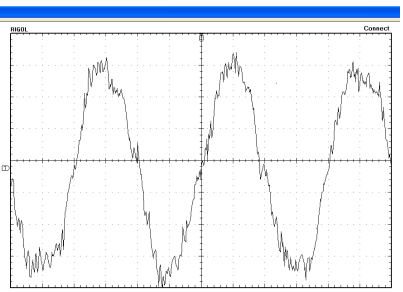

Figure 9(c).

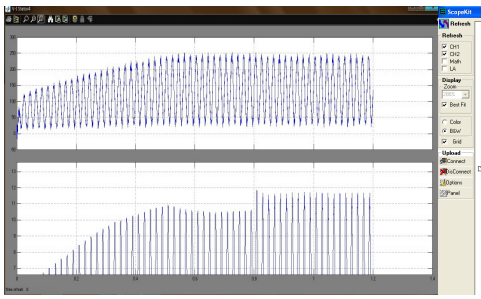

Figure 9(b).

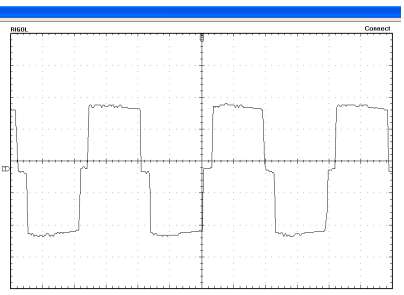

Figure 9(d).

Figure 9. Simulated and Experimenal waveforms

VII. CONCLUSIONS

This paper proposes a fuzzy logic controller suitable for solar and wind hybrid energy conversion for isolated applications. The variations in duty-cycle to maintain constant load voltage with variations in irradiation and wind speed is achieved with the proposed fuzzy logic controller with optimized rule-base. Using the mathematical model described the photo-voltaic, dynamic and steady-state characteristics are discussed. The simulated and experimental waveforms are focused on both the steady-state and dynamic behaviour which demonstrate the validity of the proposed model. The experimental result of hybrid scheme indicates the dual objectives of inherent power balance and load voltage control.

ACKNOWLEDGEMENTS

The authors thank the authorities of Annamalai University for the facilities provided.

REFERENCES

[1]. B. Ravichandra Rao and R. Amala LollyFuzzy (2012) "Fuzzy control of squirrel cage induction machine and wind generation system", International Journal of Advances in Engineering and Technology, Vol.2, no.1, pp 159-167.

[2]. S.Meenakshi, K.Rajambal, C.Chellamuthu, S.Elangovan, (2006) "Intelligent Controller for Stand-Alone Hybrid Generation System", *Power India Conference IEEE,* pp 8-15.

[3]. Ashraf A.Ahmed, Li Ran, Jim Bumby, (2008) "Simulation and control of a Hybrid PV-Wind System", *Power Electronics Machines & Drives, PEMD 4th IET conference*, pp 421-425.

[4]. WeiQi, Jinfeng Liu, Xianzhong Chen, Panagiotis D. Christofides (2011) "Supervisory predictive control of standalone wind/solar energy generation system",*IEEE Trans.on control system technology,*vol.19, no.1, pp 199-207.

[5]. T.Ahmed, N. Katsumi, N.Mutsuo, (2007) "Advanced control of PWM converter with variable-speed induction generator", *IET Electr.Power Appl*, pp 239-247.

[6]. S.Bhim, K.Gaurav kumar, (2008) "Solid state voltage and frequency controller for a stand- alone wind power generating system",*IEEE Trans.Power Electron*, pp 1170-1177.

[7]. B.Venkatesa perumal, K.Jayanta,(2008) "Voltage and *frequency* controller of a stand- alone brushless wind electric generation using generalized impedance controller" *IEEE Trans. Energy Convers*, pp 632-641.

[8]. S.Bhim, K.Gaurav kumar, (2008) "Voltage and frequency controller for three phase four wire autonomous wind energy conversion system", *IEEE Trans.Energy Convers,*pp 509-518.

[9]. M.G.Villalva, J.R.Gazol, and E.R.Filho, (2009) "Comprehensive Approach to Modeling and Simulation of Photovoltaic Arrays", *IEEE trans. on Power Electronics*, vol.24, no.5, pp.1198-1208.

[10]. H. Patel, and V. Agarwal, (2008) "MATLAB based modeling to study the effects of partial shading on PV array characteristics", *IEEE trans. on energy conv*., vol. 23, no.1, pp. 302-310.

[11]. T.Ahmed, Kastsumi Nishida, and Mutsuo Nakaoka, (2006) "Advanced control of PWM converter with variable-speed induction generator" *IEEE Trans.Ind.Appl,*vol.42, no.4, pp. 934-945.

[12]. A.Karthikeyan, C.Nagamani, G.Saravana Illango, A.Sreenivasulu, (2011) "Hybrid, open-loop excitation system for a wind turbine –driven stand-alone induction generator", *IET Renewable Power Generation,* Vol.5, no.2, pp.184-193.

[13]. Timothy, and J. Ross,(1997) "Fuzzy logic with engineering applications", McGraw hill international editions, Electrical engineering series, New York.

APPENDIX

A MATLAB (version 7.9.0.529) based modeling and simulation scheme along with fuzzy logic controller is proposed (Fig. 10) which are suitable for studying the steady-state and dynamic behaviour of the hybrid system. In order to achieve the load voltage constant the actual voltage fed to the inverter is compared with the reference maximum voltage that can be obtained at the load. The error is calculated and accordingly the reference signal to the PWM generator is changed in order to maintain the load voltage constant.

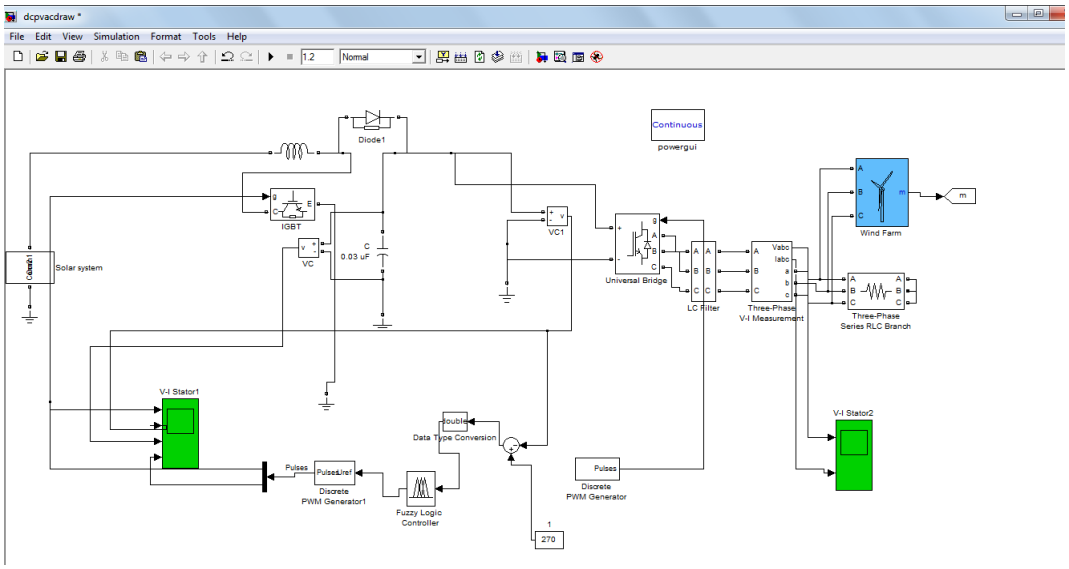

Figure 10. Hybrid solar/wind scheme with fuzzy controller in simulink (version 7.9.0.529)

Experimental setup and machine parameters

The PV array in the proposed scheme shown in Fig. 10(b) consists of solar PV array of 74.8W, 21.2V, 4.4A. A load of 80Ω per-phase was connected in star across the inverter terminals. A DC-DC converter (L=40μH, C=0.025F) was constructed with IGBT (40 A, 600 V) as a switch with a switching frequency of 2 KHz shown in Fig.10 (a). The closed loop firing scheme was employed to trigger the DC-DC converter. A 50Hz, three-phase IGBT inverter was fabricated, and a microcontroller PIC 16F877A was used to trigger the IGBT in 180 degree conduction mode. The above scheme was tested for different speed and load.

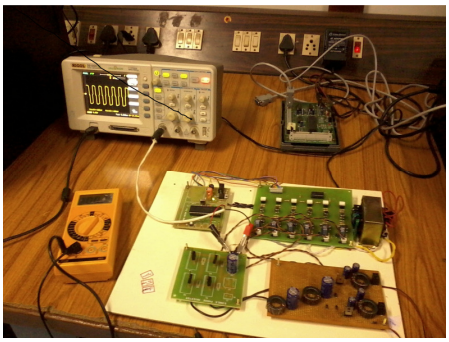

Figure 10(a): DC-DC-Converter - Inverter

Figure 10(b): Solar Panel

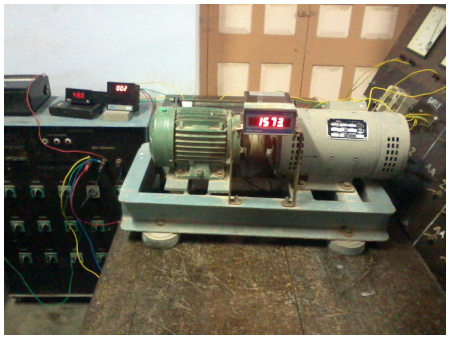

Fig 10(b): Self-Excited Induction generator (driven by D.C motor for variable speed)

Details of Experimental setup

Specifications of the Induction Machine, three-phase, 50 Hz, four-pole, 415V, 2A, 0.75 kW

Machine parameters in per-phase

Stator resistance $R_S = 9.1\Omega$
Rotor resistance $R_r = 11.8\Omega$
Stator and rotor leakage reactance
$X_{ls} = X_{lr} = 11.9\Omega$

Magnetisation curve – linearized as

$V_g/a = 260.68 - 0.523X_M$, $X_M \leq 140$
$V_g/a = 410.81 - 1.5415X_M$, $X_M > 140$

Authors

G.Balasubramanian received Bachelor of Engineering in Electrical and Electronics Engineering in 2000, Master of Engineering in Power System Engineering in 2005 from Annamalai University, Annamalainagar, Tamilnadu, India. He is Assistant Professor in the Electrical Engineering department at Annamalai University. He is currently pursing Ph.D degree in the Department of Electrical Engineering, Annamalai University.His research interests are in electrical machines, power systems, power electronics, solar and wind energy applications.

S.Singaravelu received Bachelor of Engineering in Electrical and Electronics Engineering in 1990, Master of Engineering in Power System Engineering in 1992 and Ph.D in 2007 from Annamalai University, Annamalainagar, Tamilnadu, India. He is Associate Professor in the Department of Electrical Engineering at Annamalai University. His research interests are in power electronics, power systems, electrical machines, wind/solar energy applications and high voltage DC transmission.